Journal of Molecular Catalysis A: Chemical 300 (2009) 103–110

Contents lists available at ScienceDirect

Journal of Molecular Catalysis A: Chemical

journal homepage: www.elsevier.com/locate/molcata

Role of yttrium loading in the physico-chemical properties and soot combustion activity of ceria and ceria–zirconia catalysts

I. Atribak, A. Bueno-López*, A. García-García

MCMA Group, Department of Inorganic Chemistry, University of Alicante, Ap.99 E-03080, Alicante, Spain

ARTICLE INFO

Article history:
Received 26 May 2008
Received in revised form 30 October 2008
Accepted 30 October 2008
Available online 6 November 2008

Keywords:
Soot
Ceria
Zirconia
Yttrium
Mixed oxide

ABSTRACT

$Ce_{1-x}Y_xO_2$ and $Ce_{0.85-x}Zr_{0.15}Y_xO_2$ mixed oxides have been prepared by 1000 °C-nitrates calcination to ensure thermally stable catalysts. The physico-chemical properties of the mixed oxides have been studied by N_2 adsorption at −196 °C, XPS, XRD, Raman spectroscopy and H_2-TPR, and the catalytic activity for soot oxidation in air has been studied by TG in the loose and tight contact modes. Yttrium is accumulated at the surface of $Ce_{1-x}Y_xO_2$ and $Ce_{0.85-x}Zr_{0.15}Y_xO_2$, and this accumulation is more pronounced for the former formulation than for the latter, because the deformation of the lattice due to zirconium doping favours yttrium incorporation. Yttrium and zirconium exhibit opposite effects on the surface concentration of cerium; while zirconium promotes the formation of cerium-rich surfaces, yttrium hinders the accumulation of cerium on the surface. For experiments in tight contact between soot and catalyst, all the $Ce_{1-x}Y_xO_2$ catalysts are more active than bare CeO_2, and $Ce_{0.99}Y_{0.01}O_2$ is the most active catalyst. The benefit of yttrium doping in catalytic activity of ceria can be related to two facts: (i) the Y^{3+} surface enrichment hinders crystallite growth; (ii) the surface segregation of Y^{3+} promotes oxygen vacancies creation. High yttrium loading ($x = 0.12$) is less effective than low dosage ($x = 0.01$) because yttrium is mainly accumulated at the surface of the particles and hinders the participation of cerium in the soot oxidation reaction, which is the active component. For the mixed oxides with formulation $Ce_{0.85-x}Zr_{0.15}Y_xO_2$ (operating in tight contact) the effect of zirconium on the catalytic activity prevails with respect to that of yttrium. For experiments in loose contact between soot and catalyst, the catalytic activity depends on their BET surface area, and the catalysts $Ce_{0.85-x}Zr_{0.15}Y_xO_2$ (BET = 10–13 m^2/g) are more active than the catalysts $Ce_{1-x}Y_xO_2$ (BET = 2–3 m^2/g). In the loose contact mode, the yttrium doping and loading have a minor or null affect on the activity, and the stabilising effect of the BET area due to zirconium doping prevails.

1. Introduction

Diesel engines are widely used due to their superior efficiency, durability and reliability. Particularly, the penetration of the Diesel engine into the light-duty and passenger cars exceeds 50% market share in several European countries [1]. In recent years, increasing attention has been paid to Diesel engine emissions, especially the particulate matter fraction (PM), consisting mostly of carbonaceous soot and a volatile organic fraction of hydrocarbons condensed or adsorbed over the soot, which is highly hazardous due to its potential mutagenic and carcinogenic activity [2,3]. In particular, Diesel PM smaller than 2.5 μm (PM2.5) does not only penetrate deep in the lungs but remains there longer than larger particles. Consequently, the formulation of restrictive legislation in EU regarding these fine particles is being imposed [4].

The use of a multifunctional catalytic filter combining high efficiency in PM filtration and oxidation of the captured PM seems to be the most plausible after-treatment strategy in this context [5], and intense research efforts are being currently focussed on the development of catalytic active phases that fulfil the requirements of such application.

For the last 25 years, ceria-based catalytic materials have demonstrated to be effective for three way catalysts (TWCs), which have been successfully implemented in gasoline vehicles for simultaneous CO, hydrocarbons and NOx removal. The role of ceria as an efficient oxygen buffer is directly related to its capability to undergo reduction and reoxidation under fuel-rich and lean conditions, respectively [6]. A major drawback of CeO_2 is that significant deactivation occurs due to particle sintering when it is used at high temperatures in the driving conditions. To overcome this handicap, CeO_2-based binary and ternary mixed oxides with improved thermal stability have been developed. The modification of CeO_2 by doping with transition or rare earth metals, such as Zr^{4+}, La^{3+}, Y^{3+} or Sm^{3+} among others, is likely to stabilise the surface area, to

* Corresponding author. Tel.: +34 96 590 3400x2226; fax: +34 96 590 3454.
E-mail address: agus@ua.es (A. Bueno-López).

1381-1169/$ – see front matter © 2008 Elsevier B.V. All rights reserved.
doi:10.1016/j.molcata.2008.10.043

improve the redox properties of ceria and to prevent the decline of oxygen storage capacity (OSC) due to thermal deactivation [7,8].

Recently, the promising activity of doped-CeO_2 catalysts for soot oxidation has been reported [8–12]. La^{3+}-doped CeO_2 showed improved catalytic activity for soot oxidation in comparison with bare CeO_2, and among a set of $Ce_xLa_{1-x}O_2$ mixed oxides with different La^{3+} loading ($0 < x < 0.5$), the best catalytic performance was attained with 5–10% La^{3+} ($x = 0.05$–0.10) [13]. Several rare earth-doped CeO_2 mixed oxides, with 10% foreign cation loading, were prepared afterwards [8], and $Ce_{0.9}Pr_{0.1}O_2$ and $Ce_{0.9}La_{0.1}O_2$ catalysts showed superior soot oxidation activity compared with $Ce_{0.9}Sm_{0.1}O_2$ and $Ce_{0.9}Y_{0.1}O_2$. The effect of praseodymium loading was then investigated [12] in $Ce_xPr_{1-x}O_2$ catalysts, and the best activity was obtained with 1:1 Ce:Pr molar ratio ($x = 0.5$). The catalytic activity for soot oxidation of ceria–zirconia mixed oxides, $Ce_xZr_{1-x}O_2$ with $0.5 < x < 1$, has been also studied [14] and, in this case, no differences were found in soot oxidation catalytic activity due to zirconium loading. Thus, the choice of the dopant and its amount may critically affect phase stability of the product and other features that affect the catalytic activity for soot oxidation.

The scarcity of systematic studies in the literature does not allow a rationale for the role of the dopant in modifying the textural, phase stability and catalytic activity of CeO_2-based catalysts for soot oxidation. The synthesis route plays a critical role in determining the properties of these doped systems and, very often, the effect of dopants can be masked by the fact that samples with different textural properties are compared [15]. On the other hand, most studies focussed on the development of CeO_2-based mixed oxides for catalysed soot oxidation have been performed with binary mixed oxides and few ones with ternary systems [10]. Taking this idea into account, it has been decided to analyse both binary ($Ce_{1-x}Y_xO_2$) and ternary ($Ce_{0.85-x}Zr_{0.15}Y_xO_2$) systems in the current study.

In particular, the present study aims at the effect of the yttrium loading over ceria and ceria–zirconia mixed oxides on the physicochemical properties of the resultant catalysts as well as the activity for soot combustion under tight and loose soot–catalyst contact modes. High calcination temperature (1000 °C) was selected to prepare the mixed oxides, since thermal stability is a requirement for this application taking into account the high temperature eventually reached in the Diesel Particulate Filters (DPFs) during regeneration [16], leading to low surface area materials. Besides, the surface areas of the catalysts prepared at 1000 °C are very similar to each other, allowing us a better interpretation of the influence of the dopant amount. This paper ties in with a previous publication [14] where ceria–zirconia mixed oxides calcined at 1000 °C were revealed as more active catalysts for soot combustion than bare ceria.

2. Experimental

2.1. Catalyst preparation

Catalysts of nominal composition $Ce_{1-x}Y_xO_2$ and $Ce_{0.85-x}Zr_{0.15}Y_xO_2$ (x ranging from 0 to 0.12 molar fraction) were prepared from $Ce(NO_3)_3{\cdot}6H_2O$, $ZrO(NO_3)_2{\cdot}xH_2O$ and $Y(NO_3)_3{\cdot}6H_2O$ (Aldrich, 99.9% purity) as precursors. The required amounts of these precursors were mixed in a mortar and calcined in static air at 1000 °C for 90 min (heating rate 10 °C/min). The nomenclature of the catalysts prepared is compiled in Table 1. For the sake of simplicity, 2 is kept as oxygen coefficient in the formulas $Ce_{1-x}Y_xO_2$ and $Ce_{0.85-x}Zr_{0.15}Y_xO_2$ (which is the formal coefficient in bare ceria and ceria–zirconia mixtures) despite lower values are expected due to the partial substitution of Ce^{4+} by Y^{3+}.

Table 1
Catalyst characterisation by XRD and N_2 adsorption at −196 °C.

Catalyst	Phase	Average crystal size (nm)	BET (m^2/g)
CeO_2	Cubic (c)	110	2
$Ce_{0.99}Y_{0.01}O_2$	Cubic (c)	101	2
$Ce_{0.94}Y_{0.06}O_2$	Cubic (c)	93	3
$Ce_{0.88}Y_{0.12}O_2$	Cubic (c)	90	2
$Ce_{0.85}Zr_{0.15}O_2$	Cubic (c)	93	11
$Ce_{0.84}Zr_{0.15}Y_{0.01}O_2$	Cubic (c)	46	13
$Ce_{0.80}Zr_{0.15}Y_{0.05}O_2$	Cubic (c)	51	12
$Ce_{0.75}Zr_{0.15}Y_{0.10}O_2$	Cubic (c)	45	10

2.2. Catalyst characterisation

The BET surface area of the catalysts was determined by physical adsorption of N_2 at −196 °C in an automatic volumetric system (Autosorb-6, Quantachrome).

Powder X-ray diffraction patterns were collected on a Bruker D8 diffractometer using CuK_α radiation ($\lambda = 0.15418$ nm). Spectra were recorded between 10° and 60° (2θ) with a step of 0.02 and a time per step of 3 s. The average crystal sizes (D) were determined using the Williamson–Hall's equation (WH):

$$\beta_{Total} = \beta_{Size} + \beta_{Strain} = \frac{0.9 \cdot \lambda}{D \cdot \cos\theta} + \frac{4 \cdot (\Delta d) \cdot \sin\theta}{d \cdot \cos\theta} \quad (1)$$

λ is the X-ray wavelength, β_{Total} is defined as the width at half maximum of the peak, θ is the position (angle) of the peak, and Δd is the difference of the d spacing corresponding to a typical peak. A plot of $\beta_{Total}{\cdot}\cos\theta$ against $4{\cdot}\sin\theta$ yields the average crystal size from the intercept value. For mixed oxides, the Williamson–Hall's equation provides a better estimation of the crystal size than the popular Scherrer's equation, since separates the effects of size and strain on the peak broadening.

Raman spectra were acquired with a Bruker RFS 100/S Fourier Transform Spectrometer using a variable power Nd:YAG laser source (1064 nm). 64 scans at 85 mW laser power (70 mW on the sample) were recorded and no heating of the sample was observed under these conditions.

XPS characterisation of the catalysts was carried out in a VG-Microtech Multilab electron spectrometer using a MgK_α (1253.6 eV) radiation source. To obtain the XPS spectra, the pressure of the analysis chamber was maintained at 5×10^{-10} mbar. The binding energy (BE) and the kinetic energy (KE) scales were adjusted by setting the C1s transition at 248.6 eV, and BE and KE values were determined with the Peak-fit software of the spectrometer. The electronic transitions $Zr_{3d5/2}$, $Y_{3d5/2}$, $Ce_{3d5/2}$, $Ce_{3d3/2}$, and the satellite cerium peak centred at 917 eV were used to determine the surface concentration of zirconium, yttrium and cerium. The proportion of Ce^{3+} cations with regard to the total cerium was calculated as the ratio of the sum of the intensities of the u^0, u', v^0, and v' bands to the sum of the intensities of all the bands [17]:

$$Ce^{3+}(\%) = \frac{v^0 + v' + u^0 + u'}{\Sigma(v + u)} \quad (2)$$

Experiments of Temperature Programmed Reduction with H_2 (H_2-TPR) were carried out in a tubular quartz reactor coupled to a TCD analyser for H_2 consumption monitoring. The experiments were conducted with 50 mg of catalyst and 30 ml/min flow of 7.7 vol.% H_2 in Ar. The heating rate was 10 °C/min.

2.3. Catalysed soot oxidation experiments

Catalytic tests were performed in a thermobalance (TA Instruments, model SDT 2960) with soot:catalyst mixtures of 1:4 weight ratio. Considering that contact between soot and catalyst is a key

Table 2
Nominal compositions and XPS-determined surface compositions of the catalysts.

Catalyst	Y/(Y + Ce + Zr) nominal atomic ratio	Y/(Y + Ce + Zr) surface atomic ratio	Ce/(Y + Ce + Zr) nominal atomic ratio	Ce/(Y + Ce + Zr) surface atomic ratio	(Ce/Zr) nominal atomic ratio	(Ce/Zr) surface atomic ratio	Ce^{3+} (%)
CeO_2	0.00	0.00	1.00	1.00	–	–	30.2
$Ce_{0.99}Y_{0.01}O_2$	0.01	0.06	0.99	0.94	–	–	29.1
$Ce_{0.94}Y_{0.06}O_2$	0.06	0.17	0.94	0.83	–	–	29.5
$Ce_{0.88}Y_{0.12}O_2$	0.12	0.28	0.88	0.72	–	–	30.7
$Ce_{0.85}Zr_{0.15}O_2$	0.00	0.00	0.85	0.89	5.7	8.1	31.7
$Ce_{0.84}Zr_{0.15}Y_{0.01}O_2$	0.01	0.06	0.84	0.82	5.6	6.8	31.4
$Ce_{0.80}Zr_{0.15}Y_{0.05}O_2$	0.05	0.13	0.80	0.73	5.3	5.2	30.8
$Ce_{0.75}Zr_{0.15}Y_{0.10}O_2$	0.10	0.21	0.75	0.65	5.0	4.6	30.2

factor in this process [18], experiments in *loose* and *tight contact* conditions were performed. Tests in loose contact simulate the soot–catalyst contact in a DPF, while experiments in tight contact allow obtaining wider differences among catalyst activity, being useful for basic research. For loose contact experiments, soot and catalyst were mixed with a spatula, while for tight contact tests both components were intimately mixed in a mortar. The temperature was raised at 10 °C/min from room temperature until 800 °C in 100 ml/min flow of air. The model soot used is a carbon black from Degussa S.A. (Printex-U), whose physico-chemical characterisation was reported elsewhere [13].

3. Results and discussion

3.1. Textural and structural properties

The BET surface areas of the catalysts are presented in Table 1. The low surface area of CeO_2 (2 m^2/g) is reasonable, considering that the samples were prepared by thermal treatment of the nitrate precursor at high temperature (1000 °C). Regardless the yttrium loading, the surface area remains constant at 2–3 m^2/g for all the catalysts of the $Ce_{1-x}Y_xO_2$ binary series. On the contrary, Zr^{4+} doping avoids in some extent ceria sintering. The BET surface area is 11 m^2/g for $Ce_{0.85}Zr_{0.15}O_2$, and the $Ce_{0.85-x}Zr_{0.15}Y_xO_2$ ternary series presents more or less constant BET values (10–13 m^2/g). These results suggest that the BET area depends on the synthesis conditions and Zr^{4+} addition rather than to a particular yttrium loading. Different authors found opposite effects on modifying the textural stability of ceria by metal doping, either maintaining [8] or increasing [6,19–21] the BET parameter with regard to that of bare ceria. Very different preparation methods and calcination temperatures were reported in these articles leading to a great variety of surface areas and phase compositions [6,8,19,20]. This divergence in reported data accounts for the interest of this study, where very similar surface areas have been obtained for every series, thus allowing the analysis of the yttrium loading effect on the structural and catalytic properties of the samples.

The surface distribution of yttrium, zirconium and cerium on the different samples was approached by XPS measurements. The XPS-determined surface atomic ratios included in Table 2 reveal surface enrichment of yttrium in both series, $Ce_{1-x}Y_xO_2$ and $Ce_{0.85-x}Zr_{0.15}Y_xO_2$, since the surface yttrium ratios are higher than the nominal ones. The yttrium accumulation on surface is also observed in Fig. 1, which depicts the XPS-determined surface yttrium contents in terms of the nominal yttrium ones for the different catalysts. A linear correlation was found for every series with correlation coefficients of 0.9973 and 0.9993 for $Ce_xY_{1-x}O_2$ and $Ce_{0.85-x}Zr_{0.15}Y_xO_2$, respectively. All the data lie well above the auxiliary line with unity slope, evidencing yttrium accumulation on the mixed oxides surfaces. The catalyst surface enrichment with yttrium could be due to the Y^{3+} ionic radii (0.102 nm), being smaller than that of Ce^{3+} (0.114 nm) but larger than Ce^{4+} (0.097 nm) [8], thus resulting difficult a homogeneous substitution of cerium cations by yttrium cations. The heterogeneous yttrium distribution seems not to be motivated by the synthesis procedure used to prepare the samples, as verified by extracting the same data from XPS surface analysis of a $Ce_{0.60}Zr_{0.35}Y_{0.05}O_2$ sample reported by He et al. [20]. For the preparation of the mentioned sample, the co-precipitation synthesis route was used, followed by calcination at 550 °C. This sample also presents yttrium enrichment on surface, and its XPS data fit the same trends obtained with our samples (see Fig. 1).

From the data in Fig. 1 it is also deduced that the yttrium accumulation on surface is more pronounced for the $Ce_xY_{1-x}O_2$ series (slope of 1.99) than for the $Ce_{0.85-x}Zr_{0.15}Y_xO_2$ series (slope of 1.66), that is, yttrium incorporation to the Ce–Zr framework is in somehow favoured with respect to incorporation to a zirconium-free cerium oxide lattice. As discussed afterwards in the context of Raman and XRD characterisation, the CeO_2 lattice is deformed by Zr^{4+} doping, which would improve in some extent the accommodation of Y^{3+} cations within the Ce–Zr framework. The reason why yttrium surface enrichment is less pronounced in the $Ce_{0.85-x}Zr_{0.15}Y_xO_2$ series than in the $Ce_{1-x}Y_xO_2$ series could be tentatively ascribed to the fact that for the ceria-zirconia system the critical radius, that is, the cation size which gives no cell expansion upon substitution of Zr^{4+}, is very close to that of Y^{3+} (0.1102 nm) (while, for example, La^{3+} (0.1180 nm) is an oversized cation) [6,22]. This Y^{3+} substitution represents a mechanism for the release of the stress generated by insertion of the smaller Zr^{4+} into the CeO_2 lattice. At the same time, it is responsible for the high oxygen mobility in the bulk by generating mobile oxygen in the lattice itself. This hypothesis formulated by Kâspar et al. [7] seems to be valid in this context, mainly in order to explain the sequence of catalytic activity discussed below.

The XPS-determined surface atomic ratios of cerium, which are also included in Table 2 and drawn in Fig. 2, are consistent with the fact that yttrium is accumulated on the catalysts surface. All

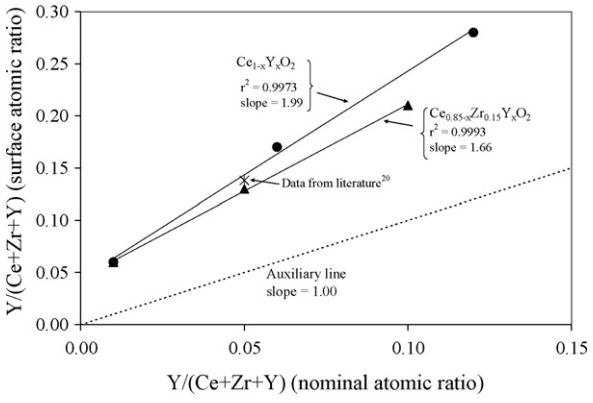

Fig. 1. XPS-determined surface atomic ratios versus nominal atomic ratios of yttrium for both series of catalysts.

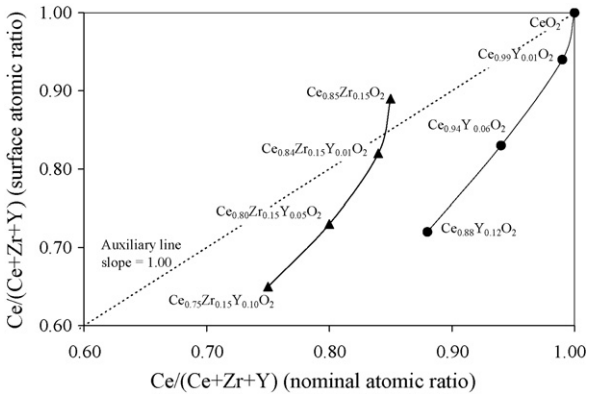

Fig. 2. XPS-determined surface atomic ratios versus nominal atomic ratios of cerium for both series of catalysts.

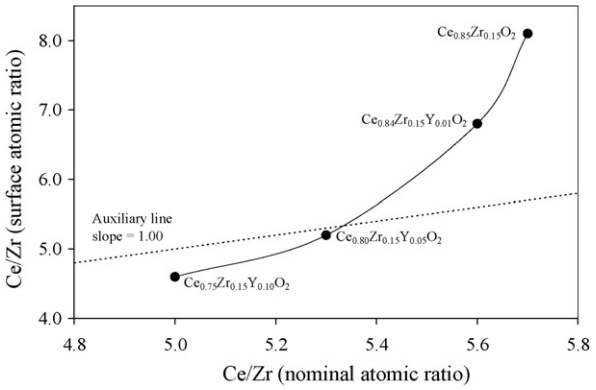

Fig. 3. XPS-determined surface Ce/Zr ratios versus Ce/Zr nominal ratios for the $Ce_{0.85-x}Zr_{0.15}Y_xO_2$ series.

the yttrium-containing catalysts present a lower cerium concentration on surface than that expected considering the nominal values, and the data of these catalysts are below the auxiliary line with slope = 1.00. Conversely, the surface cerium fraction of the sample $Ce_{0.85}Zr_{0.15}O_2$ is higher than its nominal ratio, which implies the formation of a cerium-rich phase at the periphery of the particles and a good incorporation of zirconium into the bulk. The proper dilution of zirconium on ceria is presumed by the small size of Zr^{4+} (0.084 nm), which is lower than the Ce^{4+} size (0.097 nm). It is well known that the solubility of zirconium in the crystal cell of ceria is high, and it has been reported that a cubic solid solution (either c or t″) can be maintained even up to 35 at.% zirconium [7,15]. On the contrary, other dopants present much lower solubility, being the case of yttrium, and when the solubility is low, the incorporation of the dopant may occur only at low concentrations [15]. Taking these results into account, it is deduced that yttrium and zirconium exhibit opposite effects on the surface concentration of cerium; while zirconium promotes the formation of cerium-rich surfaces, yttrium hinders the accumulation of cerium on the surface. These results must be taken into account when interpreting the catalytic properties of the mixed oxides in the last section. On one hand, CeO_2 doping with foreign cations can improve the redox properties and catalytic activity of the mixed oxides, as it has been reported [13,14], but on the other hand, the excessive depletion of cerium on surface would have a negative effect on the catalytic activity since cerium is the active component.

The Ce/Zr surface atomic ratios were also calculated from the XPS spectra and the data obtained are compiled in Table 2 along with the counterpart nominal ratios. These data are plotted in Fig. 3. For the $Ce_{0.85}Zr_{0.15}O_2$ sample, the Ce/Zr atomic ratio determined from XPS (8.1) is much higher than the corresponding nominal value (5.7). Cerium enrichment on the surface of Ce–Zr mixed oxides was also observed by other authors. Martínez-Arias et al. [23] obtained a Ce/Zr surface ratio of 2.6 for a sample with nominal composition $Ce_{0.5}Zr_{0.5}O_2$ (nominal ratio = 1) prepared by the microemulsion method. Sun and Sermon [24] also found cerium enrichment on ceria–zirconia hydrogels produced by a deposition–precipitation technique using 950 °C as calcination temperature, being the Ce/Zr surface atomic ratio of 0.25 versus a nominal composition of 0.15.

The yttrium doping also affects the Ce/Zr surface atomic ratio, as can be seen in Table 2 and Fig. 3. For the sample $Ce_{0.85}Zr_{0.15}Y_{0.05}O_2$, the surface and nominal Ce/Zr ratios are coincident, and therefore, this sample fits the auxiliary line with slope = 1.00. For lower yttrium loading (sample $Ce_{0.84}Zr_{0.15}Y_{0.01}O_2$) the measured Ce/Zr surface ratio is higher than the nominal ratio, while for higher yttrium loading ($Ce_{0.75}Zr_{0.15}Y_{0.10}O_2$) the opposite occurs. This confirms that yttrium and zirconium have opposite effects on the cation distribution throughout the mixed oxide particles, zirconium promoting cerium accumulation on surface while yttrium presenting the opposite effect.

Finally, the Ce^{3+} (surface) percentages were estimated from XPS measurements and Table 2 compiles the values obtained. As a general trend, a higher proportion of Ce^{3+} cations is detected on the $Ce_{0.85-x}Zr_{0.15}Y_xO_2$ series with regard to $Ce_xY_{1-x}O_2$ series. This behaviour is consistent with the literature, and both reducibility and segregation effects have been described for Ce–Zr mixed oxides [15]. Surface enrichment in cerium was observed in a high surface area sample with Ce:Zr ratio = 1:1, accompanied by significant cerium reduction [23].

Structural characterisation of the catalysts was carried out by means of XRD. Fig. 4a compiles the X-ray diffraction patterns for the $Ce_{1-x}Y_xO_2$ series and Fig. 4b those for the $Ce_{0.85-x}Zr_{0.15}Y_xO_2$ series. All the diffractograms show the peaks characteristic for fluorite-type structures, containing the main reflections of a material with a fcc unit cell corresponding to the (1 1 1), (2 0 0), (2 2 0), (3 1 1) and (2 2 2) planes.

The peaks of CeO_2 are narrow due to the important sintering during calcination at 1000 °C. The average crystal size estimated by the Williamson–Hall's equation (Table 1) provides a value of 110 nm for this sample. Ceria doping with Y^{3+} and/or Zr^{4+} does not provide additional reflections due to non-incorporated Y_2O_3 and/or ZrO_2.

CeO_2 doping by Y^{3+} avoids slightly ceria sintering, and the crystal sizes of the samples of the $Ce_xY_{1-x}O_2$ series gradually decrease from 101 to 90 nm with the yttrium loading, proving its stabilising effect against ceria sintering in the whole concentration range studied. The heterogeneous metal distribution on the $Ce_{1-x}Y_xO_2$ samples and the smaller crystal size of these mixed oxides with regard to bare CeO_2 are in good agreement with the thermal stabilisation effect observed by Kubsch et al. [25] in mixed oxides prepared by the co-precipitation method. CeO_2 doping with a 5% M^{3+} cations (M^{3+} = La^{3+}, Nd^{3+} and Y^{3+}, all these cations being larger than Ce^{4+}) significantly stabilised CeO_2 with respect to high temperature calcination by formation of solid solution, and M^{3+} surface enrichment was measured for these samples [25]. A common mechanism was proposed to explain this behaviour, consisting of stabilising ceria with these trivalent dopants by a surface M^{3+} enrichment that hinders ceria crystallite growth under oxidising conditions. Surface segregation of low-valence cations together with oxygen vacancies creation is energetically favoured and may stabilise the particles [25,26]. The creation of oxygen vacancies may also account for the improvement in catalytic activity towards soot combustion, as it will be discussed later. In spite of segregation of phases is not directly deduced from our XRD patterns (Fig. 4a), the possibility

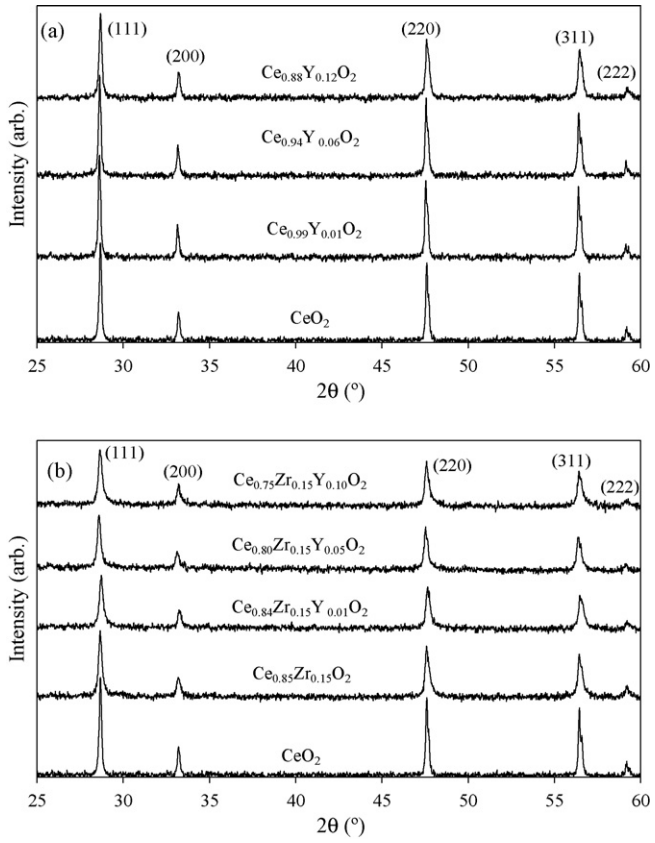

Fig. 4. X-ray diffractograms of catalysts: (a) $Ce_{1-x}Y_xO_2$ series and (b) $Ce_{0.85-x}Zr_{0.15}Y_xO_2$ series.

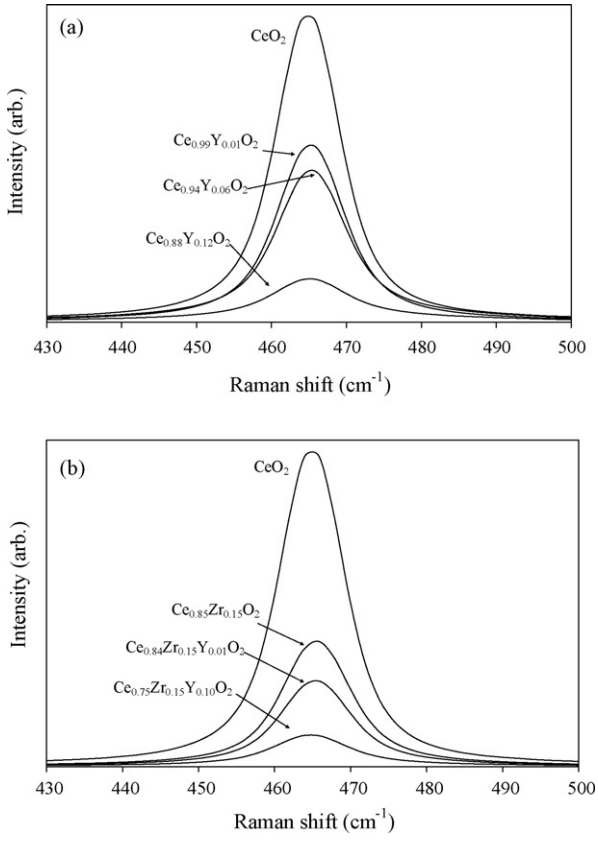

Fig. 5. Raman spectra of catalysts: (a) $Ce_{1-x}Y_xO_2$ series and (b) $Ce_{0.85-x}Zr_{0.15}Y_xO_2$ series.

which cannot be ruled out is the dispersion of YO_x on the surface of CeO_2 without forming solid solution. This segregation of phases would become more important as the yttrium loading increases from 0.01 to 0.1, and is consistent with the yttrium-rich surfaces detected by XPS analysis (see Table 2 and Fig. 1). The same conclusion was previously reported by Krishna et al. [8] for CeO_2 doped by 10% samarium or yttrium.

The crystal sizes included in Table 1 indicate that Zr^{4+} doping also prevents ceria sintering, as previously reported [15], and $Ce_{0.85}Zr_{0.15}O_2$ presents a crystal size of 93 nm versus 110 nm of ceria. The insertion of Zr^{4+} into the CeO_2 lattice remarkably modifies the sintering process and the retarding effects on the sintering rate due to Zr^{4+} addition are neatly detected by XRD technique [27].

The XRD peaks of the samples containing both zirconium and yttrium are significantly broader and their intensities are lower than those of CeO_2, $Ce_{0.85}Zr_{0.15}O_2$ and $Ce_{1-x}Y_xO_2$. This is related to the smallest crystal sizes (around 45–51 nm) of the samples of the ternary series $Ce_{0.85-x}Zr_{0.15}Y_xO_2$, and is consistent with the observed yttrium enrichment on the surface of these samples, thus avoiding crystal sintering.

Raman spectroscopy has been used to complete the structural characterisation of the samples. Fig. 5a shows the Raman spectra for the $Ce_{1-x}Y_xO_2$ series and Fig. 5b those for the $Ce_{0.85-x}Zr_{0.15}Y_xO_2$ series. The Raman spectrum of bare CeO_2 features a single band centred at 465.8 cm^{-1} that corresponds to the only allowed Raman mode (F_{2g}) of the fluorite-type structures. In contrast to XRD, which allows determining just cation sublattice symmetry, the Raman spectra provide information about oxygen anions position and reflect the oxygen lattice vibrations, being sensitive to crystalline symmetry [28].

Ceria doping by 0.01 yttrium atomic fraction leads to the F_{2g} band intensity decrease because of the framework deformation (Fig. 5a), which is in agreement with the XRD data. The F_{2g} band is progressively seen more attenuated as the Y^{3+} loading increases, but without peak position shift. It has been reported [6] that the deformation induced by the dopants favours oxygen mobility.

The incorporation of Zr^{4+} into the ceria lattice also produces a structural distortion, as inferred by the decrease in the F_{2g} band intensity of the zirconium-containing samples regarding to CeO_2 (Fig. 5b). From the comparison of the decrease in the band intensities of $Ce_{0.88}Y_{0.12}O_2$ and $Ce_{0.85}Zr_{0.15}O_2$ with regard to bare CeO_2 is deduced that Y^{3+} affects the oxygen vibration more than Zr^{4+} does. As mentioned, CeO_2 doping by Y^{3+} doping requires oxygen removal from mixed oxide structure and creation of vacant sites to maintain the net zero charge of the frame. On the contrary, the distortion of oxygen vibrations by Zr^{4+} doping is mainly a matter of cationic sizes, and thus, it has less effect on vacant creation than Y^{3+}. From a qualitative point of view, the introduction of Y^{3+} in the Ce–Zr mixed oxide (Fig. 5b) does not produce such an important decline in the band intensity as Y^{3+} doping does in ceria (Fig. 5a).

3.2. Redox properties

H_2-TPR experiments were performed to analyse the reducibility of the catalysts, and the H_2-consumption profiles obtained are plotted in Fig. 6. As observed, the TPR behaviour appears to be governed both by textural and structural properties of the samples.

It is generally accepted that the reduction profile of CeO_2 presents two peaks attributed to the surface and bulk Ce^{4+} reduction [19], respectively. In Fig. 6, only the bulk reduction peak centred at 840 °C is observed for the catalyst CeO_2, and the surface

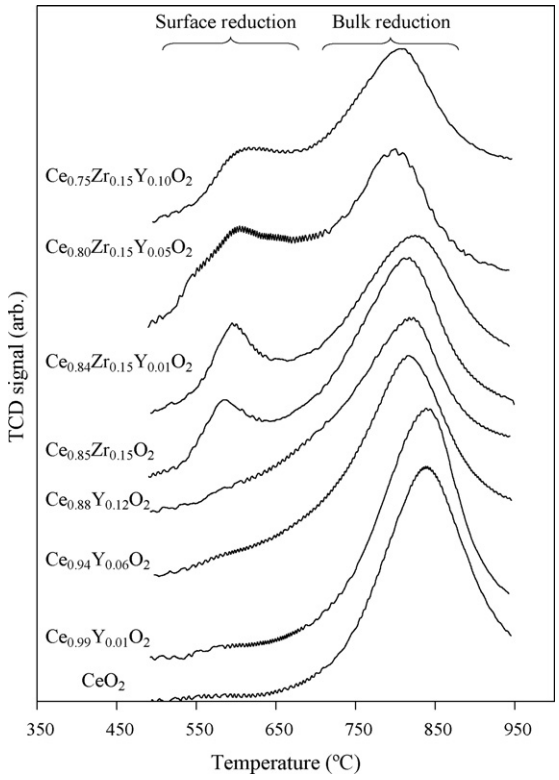

Fig. 6. H_2-consumption profiles during H_2-TPR experiments.

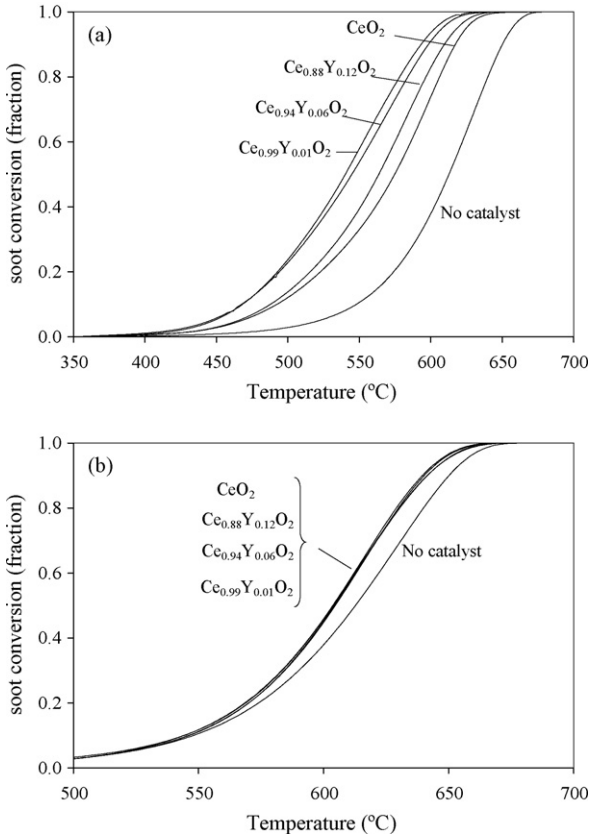

Fig. 7. Soot conversion profiles versus temperature for $Ce_{1-x}Y_xO_2$ series: (a) tight contact and (b) loose contact.

reduction peak is not detected in accordance with the low surface area of this sample (2 m^2/g). An identical profile is obtained with the sample $Ce_{0.99}Y_{0.01}O_2$, suggesting that the incorporation of a very low amount of yttrium does not influence the bulk reduction process. The position of the bulk reduction peak shifts slightly from 840 °C for CeO_2 and $Ce_{0.99}Y_{0.01}O_2$ to 815 °C for $Ce_{0.94}Y_{0.06}O_2$ and $Ce_{0.88}Y_{0.12}O_2$, indicating that a minimum yttrium level (between 0.01 and 0.06) is necessary to obtain a moderate improvement in the bulk reduction. Vidmar et al. [6] found similar trends when comparing the reduction behaviour of $Ce_{0.6}Zr_{0.4-x}Y_xO_{2-x/2}$ samples, reporting that the shape in the TPR profile was not modified by doping with 1 mol% in Y^{3+}, and by increasing the Y^{3+} content up to 5 mol%, the maximum of the bulk reduction peak shifted down 26 °C, in agreement with our results.

The zirconium-containing samples show two H_2-consumption peaks, the bulk reduction peak centred around 800–850 °C, depending on the sample, and another peak around 500–625 °C due to surface reduction. This is in agreement with the higher surface area of the zirconium-containing catalysts (10–13 m^2/g) in contrast with those without zirconium (2–3 m^2/g). Taking a close look to the H_2-consumption profiles of the zirconium-containing samples it is possible to realise that there is consumption of H_2 in the range of temperatures between the peaks attributed to surface and bulk reduction. This means that both processes do not occur independently to each other, but the bulk oxygen is pumped out to the surface as the surface oxygen is depleted, and is a good evidence of the oxygen mobility within the lattice. It has been calculated from atomistic simulation that the energy for the Ce^{4+} reduction to Ce^{3+} in $Ce_xZr_{1-x}O_2$ solid solutions is comparable to that calculated for the CeO_2 surface [29]. Certain oxygen mobility can be inferred from the H_2-consumption profiles of the $Ce_{0.85}Zr_{0.15}O_2$ and $Ce_{0.84}Zr_{0.15}Y_{0.01}O_2$ samples, and this mobility is enhanced for $Ce_{0.80}Zr_{0.15}Y_{0.05}O_2$ and $Ce_{0.75}Zr_{0.15}Y_{0.10}O_2$ suggesting a synergetic effect of Zr^{4+} and Y^{3+} doping in this behaviour.

3.3. Catalytic activity and overall discussion

The soot conversion profiles corresponding to the catalytic tests performed with the series $Ce_{1-x}Y_xO_2$ and $Ce_{0.85-x}Zr_{0.15}Y_xO_2$ are included in Figs. 7 and 8, respectively. In both cases, experiments in soot–catalyst tight contact (Figs. 7a and 8a) and loose contact (Figs. 7b and 8b) are compared. In Table 3, the temperatures at which a 50% of soot is consumed in each experiment are compiled.

Remarkable differences are observed between the profiles in Fig. 7a and b. Under the loose contact mode (Fig. 7b) the four catalysts behave in the same manner, according to their similar and low surface areas (2–3 m^2/g). When the contact between soot and catalyst is poor, only the number of contact points seems to be crucial for the catalytic activity, much more than their chemical nature or surface status (vacant sites concentration, yttrium and cerium surface concentration, or oxygen mobility). In loose contact conditions the BET surface area of the catalyst plays the most important role

Table 3
Temperature for 50% soot conversion (T50%) in soot oxidation tests.

Catalyst	T50% (°C) loose contact	T50% (°C) tight contact
CeO_2	605	575
$Ce_{0.99}Y_{0.01}O_2$	604	540
$Ce_{0.94}Y_{0.06}O_2$	604	545
$Ce_{0.88}Y_{0.12}O_2$	604	564
$Ce_{0.85}Zr_{0.15}O_2$	597	471
$Ce_{0.84}Zr_{0.15}Y_{0.01}O_2$	593	456
$Ce_{0.80}Zr_{0.15}Y_{0.05}O_2$	597	470
$Ce_{0.75}Zr_{0.15}Y_{0.10}O_2$	595	470

T50% for uncatalysed reaction = 613 °C.

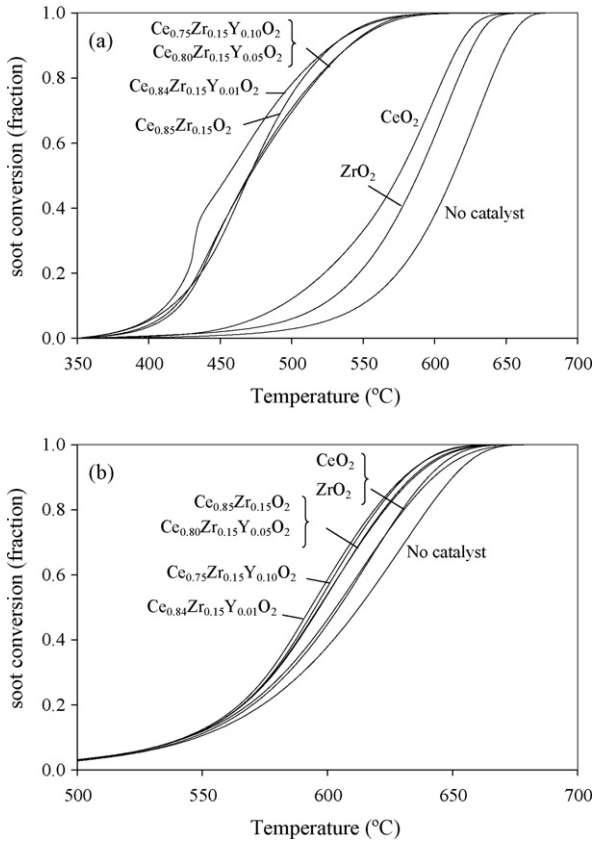

Fig. 8. Soot conversion profiles versus temperature for $Ce_{0.85-x}Zr_{0.15}Y_xO_2$ series: (a) tight contact and (b) loose contact.

in the catalytic activity for soot combustion, as reported by other authors [8].

Performing the reactions under tight contact is interesting in order to screen the efficiency of the catalysts and establishing correlations with their physico-chemical features. As shown in Fig. 7a, all the $Ce_{1-x}Y_xO_2$ catalysts are more active than bare CeO_2, and $Ce_{0.99}Y_{0.01}O_2$ is the most active catalyst of this series decreasing the T50% temperature by 73 and 35 °C with regard to the uncatalysed and CeO_2-catalysed reactions, respectively. The catalytic activity of $Ce_{0.94}Y_{0.06}O_2$ is only slightly lower to that of $Ce_{0.99}Y_{0.01}O_2$, but increasing the yttrium atomic ratio to 0.12 has a negative effect on the activity with respect to lower yttrium loading. This trend in activity can be understood according to the surface composition of the $Ce_{1-x}Y_xO_2$ samples. As deduced from XPS, yttrium is mainly accumulated at the particles surface, and a progressive decrease of the cerium amount on surface occurs by increasing the yttrium loading. This surface cerium depletion would explain the decrease in activity taking into account that cerium is the active component of the mixed oxide. The benefit of a very low yttrium dosage can be explained due to solid solution formation with M^{3+} surface segregation together with creation of oxygen vacancies. In summary, the role of yttrium on the catalytic activity of ceria depends on its loading. 0.01–0.06 loading has a positive effect on the activity because of the formation of a solid solution that enhances the cerium activity, but higher loading (0.12) is less effective because yttrium is mainly accumulated at the surface of the particles, leaving a lower proportion of cerium available to catalyse the soot oxidation reaction.

It is worth mentioning that the improvement in redox properties for the ceria–catalysts with the highest dopant contents (manifested by a shift in the bulk reduction peak from 840 to 815 °C in the H_2-TPR experiments) seems not to affect positively the soot oxidation rate. On the contrary, the activity decreases following the order: $Ce_{0.99}Y_{0.01}O_2 > Ce_{0.94}Y_{0.06}O_2 \gg Ce_{0.88}Y_{0.12}O_2 > CeO_2$ (see Fig. 7a), suggesting that a very low dosage of trivalent cation is enough to reach the maximum activity for soot combustion under these experimental conditions. Other important fact contributes to explain this trend characterised by a lack of correlation with the H_2-TPR results: the catalyst bulk reduction takes place at high temperatures, and hence, the bulk is not involved in the soot oxidation process (occurring below 700 °C). This asseveration was reported by Krishna et al. [8] for a series of ceria catalysts doped with different rare earth cations.

The behaviour of the $Ce_{0.85-x}Zr_{0.15}Y_xO_2$ catalysts (Fig. 8) presents differences in comparison with the $Ce_{1-x}Y_xO_2$ binary series (Fig. 7), and as a general trend, all the zirconium-containing catalysts are more active than those without zirconium. The zirconium-containing samples decreased the T50% temperature by 150 and 20 °C approximately, for tight and loose contact conditions, respectively, with respect to the uncatalysed combustion.

The enhanced activity of the catalysts with zirconium is a consequence of their higher BET surface area and improved redox properties (enhanced oxygen mobility and surface reducibility) in comparison with zirconium-free catalysts. The BET area of the zirconium-containing catalysts ranges from 10 to 13 m^2/g, and ensures a better soot–catalyst contact than the 2–3 m^2/g of the $Ce_{1-x}Y_xO_2$ catalysts. This is supported by the fact that the differences among the catalytic activity of the samples with composition $Ce_{0.85-x}Zr_{0.15}Y_xO_2$ are minor, while important differences in the surface composition and redox properties of these samples were described in the previous sections. In conclusion, for the mixed oxides with formulation $Ce_{0.85-x}Zr_{0.15}Y_xO_2$, the effect of zirconium on the catalytic activity prevails with respect to the effect of yttrium.

4. Conclusions

In this study, the physico-chemical properties and the catalytic activity for soot oxidation of $Ce_{1-x}Y_xO_2$ and $Ce_{0.85-x}Zr_{0.15}Y_xO_2$ mixed oxides have been analysed and the following main conclusions can be summarised:

- The XPS characterisation showed that yttrium is accumulated at the surface of the particles of both $Ce_{1-x}Y_xO_2$ and $Ce_{0.85-x}Zr_{0.15}Y_xO_2$, and this surface enrichment by yttrium is more pronounced for the $Ce_xY_{1-x}O_2$ series than for the $Ce_{0.85-x}Zr_{0.15}Y_xO_2$ series. Yttrium incorporation to the Ce–Zr framework seems to be favoured with respect to its incorporation to a zirconium-free cerium oxide lattice because of the deformation of the lattice due to zirconium doping, as deduced by XRD and Raman.
- Yttrium and zirconium exhibit opposite effects on the surface concentration of cerium; while zirconium promotes the formation of cerium-rich surfaces, yttrium hinders the accumulation of cerium on the surface.
- For experiments in tight contact between soot and catalyst, all the $Ce_{1-x}Y_xO_2$ catalysts are more active than bare CeO_2, and $Ce_{0.99}Y_{0.01}O_2$ is the most active catalyst. The benefit of yttrium doping in catalytic activity of ceria can be related to two facts: (i) the Y^{3+} surface enrichment hinders crystallite growth; (ii) the surface segregation of Y^{3+} promotes oxygen vacancies creation. High yttrium loading ($x = 0.12$) is less effective than low dosage ($x = 0.01$) because yttrium is mainly accumulated at the surface of the particles and hinders the participation of cerium in the soot oxidation reaction, which is the active component. For the mixed oxides with formulation $Ce_{0.85-x}Zr_{0.15}Y_xO_2$, the effect of

zirconium on the catalytic activity prevails with respect to that of yttrium.

- For experiments in loose contact between soot and catalyst, the catalytic activity depends on the BET surface area of the catalyst, and the catalysts $Ce_{0.85-x}Zr_{0.15}Y_xO_2$ (BET = 10–13 m^2/g) are more active than the catalysts $Ce_{1-x}Y_xO_2$ (BET = 2–3 m^2/g). In the loose contact mode, the yttrium doping and loading have a minor or null affect on the activity, and the stabilising effect of the BET area due to zirconium doping prevails.

Acknowledgments

The authors thank the financial support of the Spanish Ministry of Education and Science by funding the project MAT2006-12635 and the contract of ABL (Ramon y Cajal Program), which is co-funded by Generalitat Valenciana and University of Alicante.

References

[1] Y. Zhang, X. Zou, F. Yu, J. Xu, Appl. Catal. B 77 (2007) 79–91.
[2] D. Fino, E. Cauda, D. Mescia, N. Russo, G. Saracco, V. Specchia, Catal. Today 119 (2007) 257–261.
[3] N.E. Olong, K. Stöwe, W.F. Maier, Appl. Catal. B 74 (2007) 19–25.
[4] http://www.solociencia.com/ecologia/05042108.htm.
[5] M.L. Pisarello, V. Milt, M.A. Peralta, C.A. Querini, E.E. Miró, Catal. Today 75 (2002) 465–470.
[6] P. Vidmar, P. Fornasiero, J. Kâspar, G. Gubitosa, M. Graziani, J. Catal. 171 (1997) 160–168.
[7] J. Kâspar, P. Fornasiero, M. Graziani, Catal. Today 50 (1999) 285–298.
[8] K. Krishna, A. Bueno-López, M. Makkee, J.A. Moulijn, Appl. Catal. B 75 (2007) 189–200.
[9] E. Aneggi, M. Boaro, C. de Leitenburg, G. Dolcetti, A. Trovarelli, Catal. Today 112 (2006) 94–98.
[10] E. Aneggi, C. de Leitenburg, G. Dolcetti, A. Trovarelli, Catal. Today 114 (2006) 40–47.
[11] K. Krishna, A. Bueno-López, M. Makkee, J.A. Moulijn, Appl. Catal. B 75 (2007) 201–209.
[12] K. Krishna, A. Bueno-López, M. Makkee, J.A. Moulijn, Appl. Catal. B 75 (2007) 210–220.
[13] A. Bueno-López, K. Krishna, M. Makkee, J.A. Moulijn, J. Catal. 230 (2005) 237–248.
[14] I. Atribak, A. Bueno-López, A. García-García, Catal. Commun. 9 (2008) 250–255.
[15] A. Trovarelli, Catalytic Science Series, vol. 2, Imperial College Press, 2002.
[16] N. Miyakawa, H. Sato, H. Maeno, H. Takahashi, JSAE Rev. 24 (2003) 269–276.
[17] A. Laachir, V. Perrichon, A. Badri, J. Lamotte, E. Catherine, J.C. Lavalley, J. El Fallal, L. Hilaire, F. le Normand, E. Quéméré, G.N. Sauvion, O.J. Touret, Chem. Soc. Faraday Trans. 87 (1991) 1601–1609.
[18] B.A.A.L. Van Setten, J.M. Schouten, M. Makkee, J.A. Moulijn, Appl. Catal. B 28 (2000) 153–257.
[19] G.L. Markaryan, L.N. Ikryannikova, G.P. Muravieva, A.O. Turakulova, B.G. Kostyuk, E.V. Lunina, V.V. Lunin, E. Zhilinskaya, A. Aboukais, Colloids Surf. A 151 (1991) 435–447.
[20] H. He, H.X. Dai, L.H. Ng, K.W. Wong, C.T. Au, J. Catal. 206 (2002) 1–13.
[21] G. Jiaxiu, Y. Shushua, G. Maochu, S. Mei, Z. Junbo, C. Yaoqiang, J. Rare Earths 25 (2007) 179–183.
[22] K. Yamada, H. Tanaka, M. Yamamoto, in SAE Technical Paper Series, (1997) 970464.
[23] A. Martínez-Arias, M. Fernández-García, V. Ballesteros, L.N. Salamanca, J.C. Conesa, C. Otero, J. Soria, Langmuir 15 (1999) 4796–4802.
[24] Y. Sun, P.A. Sermon, J. Mater. Chem. 6 (1996) 1025–1029.
[25] J.E. Kubsch, J.S. Rieck, N.D. Spencer, Catalysis and Automotive Pollution Control II, Elsevier, Amsterdam, 1991, p. 125.
[26] P.G. Harrison, D.A. Creaser, B.A. Wolfindale, K.C. Waugh, M.A. Morris, W.C. Mackrodt, Catalysis and Surface Characterisation, The Royal Society of Chemistry, Cambridge, 1996, p. 76.
[27] J. Kâspar, P. Fornasiero, R. Balducci, R. Di Monte, N. Hickey, V. Sergo, Inorg. Chim. Acta 349 (2003) 217–226.
[28] M. Fernández-García, A. Martínez-Arias, A. Iglesias-Juez, C. Belver, A.B. Hungría, J.C. Conesa, J. Soria, J. Catal. 194 (2000) 385–392.
[29] P. Li, I.W. Chen, J.E. Penner-Hahn, J. Am. Ceram. Soc. 77 (1994) 118–128.